HIPPOCAMPUS, VOL. 3, NO. 3, PAGES 317–330, JULY 1993

Phase Relationship Between Hippocampal Place Units and the EEG Theta Rhythm

John O'Keefe and Michael L. Recce

Department of Anatomy and Developmental Biology, University College London, London, U.K.

ABSTRACT

Many complex spike cells in the hippocampus of the freely moving rat have as their primary correlate the animal's location in an environment (place cells). In contrast, the hippocampal electroencephalograph theta pattern of rhythmical waves (7–12 Hz) is better correlated with a class of movements that change the rat's location in an environment. During movement through the place field, the complex spike cells often fire in a bursting pattern with an interburst frequency in the same range as the concurrent electroencephalograph theta. The present study examined the phase of the theta wave at which the place cells fired. It was found that firing consistently began at a particular phase as the rat entered the field but then shifted in a systematic way during traversal of the field, moving progressively forward on each theta cycle. This precession of the phase ranged from 100° to 355° in different cells. The effect appeared to be due to the fact that individual cells had a higher interburst rate than the theta frequency. The phase was highly correlated with spatial location and less well correlated with temporal aspects of behavior, such as the time after place field entry. These results have implications for several aspects of hippocampal function. First, by using the phase relationship as well as the firing rate, place cells can improve the accuracy of place coding. Second, the characteristics of the phase shift constrain the models that define the construction of place fields. Third, the results restrict the temporal and spatial circumstances under which synapses in the hippocampus could be modified.

Key words: place units, theta, phase correlates

Two principal types of unit can be recorded from the pyramidal cell layers of the rat hippocampus: complex spike cells and theta cells (Ranck, 1973; Fox and Ranck, 1975). The primary correlate of the first unit is the animal's location in an environment (place cells; O'Keefe and Dostrovsky, 1971; O'Keefe, 1976; Olton et al., 1978; McNaughton et al., 1983b; Muller et al., 1987), although there have also been claims that these cells respond during olfactory discrimination (Eichenbaum et al., 1986) and nictitating membrane conditioning (Berger et al., 1983). The correlate of the second type of unit, the theta unit, is less clear and may vary among species.

Place cells fire several bursts of spikes as the rat runs through one or more locations in an environment called the place field of that cell. Each burst of spikes may or may not include the complex spike pattern that is characteristic of these cells (Ranck, 1973). The place field is usually constructed by examining spike fire rates over long periods of time and therefore ignores the fine-grained temporal characteristics of the unit activity.

Conversely, the hippocampal electroencephalograph (EEG) is usually examined in the time domain. In general, the hippocampal EEG can be divided into two major classes: theta, which consists of sinusoidal 7–12 Hz waves, and large irregular activity, in which there is a broader spectrum of frequencies (Vanderwolf, 1969). The behavioral correlates of the two types of EEG vary somewhat between species (see Bland, 1986 for a recent review). In the rat, theta occurs primarily during movements that change the animal's location in the environment: walking, exploring, running, swimming, rearing, and jumping. Large irregular activity occurs during other activities—eating, drinking, and grooming—as long as these are not associated with postural shifts or other displacement movements.

Previous studies have found a phase correlation between the firing of hippocampal cells and the sinusoidal EEG theta pattern (Sinclair et al., 1982; Buzsaki et al., 1983; Fox et al., 1986; Otto et al., 1991). However, the interaction between the spatial firing of place cells and their phase locking to the theta rhythm has not adequately been resolved. In particular, the variability of rats' running speed may require some variability in either the spatial properties of the cells or the correlation to the EEG. This relationship is important in determining both the true spatial coding performed by place cells and the timing conditions for synaptic change. Recently, it has been shown that long-term potentiation preferentially occurs

Correspondence and reprint requests to Professor J. O'Keefe, Anatomy and Developmental Biology Department, University College London, Gower Street, London WC1E 6BT, U.K.

on the positive peak of the dentate theta rhythm (Pavlides et al., 1988), and there is some suggestion that the timing of the activity of pre- and postsynaptic cells determines the amount (Larson and Lynch, 1989) and possibly the direction of synaptic change (Stanton and Sejnowski, 1989).

In the present experiments we have not sought to identify the average or most likely phase correlate of the place cells, but instead have looked carefully at the relative phase changes as the rat runs through the place field. Our results show that the theta phase correlate of the place cells is not constant as the rat runs through the field, but changes in a systematic way. The first burst of firing consistently occurs at a particular phase of the reference theta, but each successive firing burst moves to a point earlier in the theta cycle. This precession of the phase correlates often continues throughout the field so that by the time the rat exits the field the phase shift may have moved through an entire cycle of the theta wave.

MATERIALS AND METHODS

Single unit and EEG recording techniques

Lister hooded rats were implanted with one or two microdrives under deep surgical anesthesia. Following induction with 3–4% halothane in nitrous oxide/oxygen, rats were mounted in a stereotactic frame and maintained on 0.5–2.0% halothane in nitrous oxide/oxygen throughout the operation, depending on the point in the procedure and the susceptibility of the individual animal. Depth of anesthesia was adjusted to keep the heart rate at 300–360 beats/minute. The skull was exposed and four or five 2.3 mm holes were drilled with a trephine drill to take stainless steel screws machined to a close tolerance. One or two 2.8 mm holes were drilled for the electrodes. Single microdrives were located over the left hippocampus (AP 3.0–4.5; L 2.0–3.5). With two microdrives, both hemispheres were used. During the implant procedure the microdrives were held in micromanipulators and the electrodes inserted into the neocortex above the hippocampus through the cut dura. The feet of the microdrives were attached to the skull screws with dental cement. The wound margins were dusted with a topical antibiotic (Cicatrin, Wellcome), and a thin layer of dental cement covered the skin to close the wound and prevent infection. Postoperative analgesia was provided by buprenorphine (Temgesic, Reckitt, and Colman, 0.15 cc, i.m.). We have independently shown that these surgical and postoperative procedures do not affect a spatial memory task known to be dependent on hippocampal integrity (O'Keefe and Speakman, 1987). Each animal was allowed to recover for several days before recording began, and no data were collected until at least 10 days postsurgery.

Microdrives, microelectrodes, and data capture

One or two small lightweight, laboratory-built microdrives were permanently implanted in each rat. Each microdrive contained two bundles of electrodes (tetrodes), one 300–500 μm above the other, in a cannula. One full rotation of the mechanical drive mechanisms produces a vertical movement of 200 μm without rotating the cannula or the electrodes.

Each tetrode is an extension of the stereotrode concept (McNaughton et al., 1983a) and consists of four Teflon-coated 25 μm platinum-iridium (90%/10%) electrodes (Recce and O'Keefe, 1989; Recce et al., 1991). These are twisted together and cut with sharpened scissors to form a tip with four exposed surfaces oriented in a rectangular or diamond-shaped pattern, each separated by the thicknesses of the Teflon insulation (2 × 3 μm thick). When located in the cell layers of the hippocampus, these tetrodes provide for simultaneous and independent measurements of the extracellular spikes from the same set of neurons. Depending on its spatial relationship to the tetrode bundle, each neuron contributes an action potential to some or all of the four channels. Figure 1 shows a schematic diagram of the technique and schematic examples of the different recording patterns that might be obtained from two complex spike cells. These patterns of action potentials are used to discriminate among the multiple spikes simultaneously recorded by the tetrode.

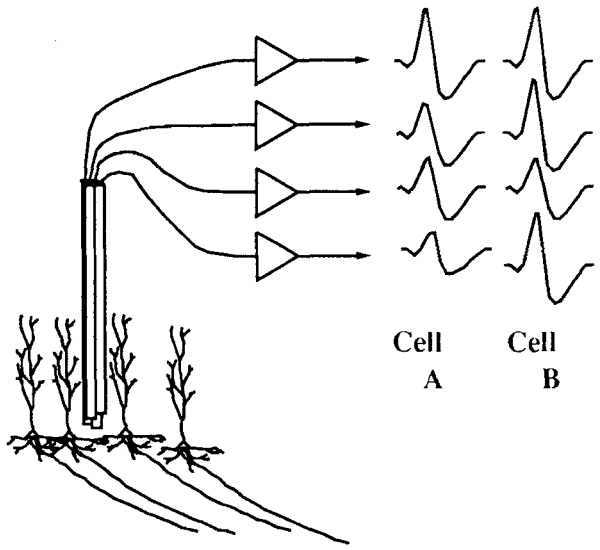

Fig. 1. Schematic diagram of the four-channel tetrode among four pyramidal cells. The signal from each channel is led to the gate of a separate dual FET. The second input to each gate comes from a single channel of a different tetrode (not shown). On the right are shown the set of action potentials that might be obtained from two different cells. Notice that the potentials on a single electrode (for example, the top row) could be identical, but the tetrode would still allow separation of these cells on the basis of differences in the signals on other channels.

Data collection

During recording, each of the four wires of each tetrode was connected to the gates of an RC-coupled FET. The eight potentials were led through long hearing-aid wires to purpose-built differential amplifiers and filters (passband 400 Hz to 5.4 kHz). Each of the four channels of one tetrode was fed into one leg of a differential amplifier. The signals for the other leg were derived from one of the channels of the other tetrode to provide a common rejection signal to minimize noise, movement, and chewing artifacts. Each channel was continuously sampled at 20 or 40 μs. When a spike event was detected

(as a voltage above a set level on any one of the channels), the sampled points around the event were stored to yield 25 or 50 points per each of 4 channels for each spike event. Each spike event was stamped with the time since the beginning of data collection and the animal's location at the time (see below). Data were usually collected in blocks of 1, 2, or 4 minutes and stored on a local hard disk.

A TV tracking system (SP111, HVS Image Analysing, Kingston, U.K.) monitored the (x, y) location of a small DC lamp on the rat's head at the frame frequency of 50 s^{-1}. These coordinates were stored with the unit data and enabled us to identify the animal's location throughout the run and to identify the location at which each spike event occurred.

The EEG data were taken either from an individual channel of the tetrode or by adding the signals from all four channels of a tetrode. Only single-ended recording was used. For some recordings the data were filtered using Neurolog variable filters (Neurolog System, Digitimer Inc., Welwyn Garden City, U.K.), but for most of the cells purpose-built EEG amplifiers and filters were used. The frequency responses of these amplifiers have been tested and found to phase shift the signal by no more than +4 ms between 1 and 20 Hz. The aim of the study was not to establish the phase correlate of each spike relative to a constant EEG standard such as the dentate theta; instead, we were more concerned with the pattern of phase shifts as the rat ran through the field. To this end we did not attempt to maintain a fixed location for the EEG reference electrodes, but instead chose whichever of the moving tetrodes yielded the best theta signal, irrespective of location. It is well established that the theta signals from different parts of the hippocampus are phase-shifted relative to each other but that this phase relation remains constant. In this report we have not attempted to assign absolute phase correlates to the place units.

In the days following recovery from surgery, the electrodes were moved down into the CA1 or CA3 pyramidal cell layers while the animal sat on a small holding platform. Once a suitable recording location was achieved, the electrodes were usually left in place for at least 1 day before data collection began in order to ensure maximum recording stability.

Behavioral testing

Each rat was weighed daily and given sufficient food to maintain weight at 90% of free-feeding weight. A 12-hour dark/light cycle was maintained with lights off at 3 P.M. Most recordings took place between 2 and 8 P.M. Units were recorded from two rats while they ran back and forth along the surface of linear tracks to obtain a reward. The tracks were 1.5 m long and either 4.6 cm or 15.2 cm wide. Reward in the form of sugar-coated cereals or sweetened rice was given at each end. Rats were trained until they ran with a consistent pattern from one end to the other. During the recording of some cells, the food reward was varied between several locations in one of the goal areas. This introduced some variability in run speed and increased the dissociation between temporal and spatial firing correlates. Additional data were taken from a third rat that was trained on an elevated plus maze in a cue-controlled environment. For further details of the procedure and response of place units in this situation, see O'Keefe and Conway (1978, 1980) and O'Keefe and Speakman (1987).

Data analysis

For off-line analysis, the data were transferred to Sun 4 workstations. Each set of tetrode data from a recording session was separated into several clusters by selecting those features of the waveforms that maximally distinguished one set of spikes from the others. It was assumed that each cluster represented the action potentials from a single neuron. In the first stage of analysis, artifact and false spike triggers were removed, using the sum of the squares of the voltage difference between each waveform and either an idealized spike or the average waveform from a clearly separated cluster. This criterion also proved effective for separating clusters from each other. Other commonly selected waveform features were the peak-to-peak amplitude and the voltage at a particular time after spike onset. In addition, automatic clustering was carried out on some of the data, using the k-means algorithm. For automatic clustering, each spike was treated as a 200-dimensional vector, in which the components are the voltages after spike onset.

Once a single spike cluster had been isolated, its firing pattern on the maze was examined. On the linear tracks, the width of the track was ignored and the place field was plotted as a firing rate along a single dimension. The 1.5 m track was divided into 64 bins of 2.34 cm each, and the number of spikes and the number of position points per run were calculated. Dividing the former by the latter gave an average firing rate per location on the maze. Runs in one direction on the track were analyzed independently from those in the opposite direction, since previous work had shown that direction of running was a major influence on mazes with narrow arms (McNaughton et al., 1983b). Sections of runs starting as the animal left one goal area and entered the other were selected. Runs containing major artifacts in either the EEG or unit records, or grossly erratic behavior by the rat, were rejected. On the plus maze, only cells with goal arm fields were included for this analysis and these were treated similarly. The justification here was that the rat tended to run in the center as it approached the goal, and there was much less lateral variation than normally occurs. The number of runs used for the different cells ranged from 11 to 115 (mean, 45.6; median, 43.5).

The place field of each cell consisted of a single block of elevated firing rate over a portion of the track. Detection of the field boundaries, therefore, was reduced to the problem of specifying at which point in space or time this block had been entered and exited. Since this is akin to the problem of detecting a pulse in the time domain, we used a similar criterion: the point at which the firing rate exceeded or fell below 10% of its maximum value. The number of bins between these points × 2.34 cm was used as the field length. The findings of the present paper suggest a second definition of the place field, at least on linear tracks, based on the phase correlate, and this is presented in the discussion section.

The correlation between unit firing and the phase of hippocampal theta rhythm was computed for each spike. For this analysis, the EEG was modeled as a set of independent sinusoidal waves, where the transition from one wave to the next

occurred near the positive to negative zero crossing. The time corresponding to this transition was computed by finding the best match between the negative half of a single-period sine wave and segments of the EEG. Each wave was extracted in sequence from the beginning of the data set. The initial half sine wave template had a wavelength of 100 ms and began at the end of the last cycle. The wavelength and the onset time of the template were changed in the direction that decreased the sum of the squares of the difference between the template and the EEG. Changes were made until no increase or decrease of 1 ms in either parameter improved the fit.

An example of the process used to find the phase of each spike is shown in Figure 2, which contains one second of data from a typical complex spike cell as the animal ran through the place field. Part A shows one vertical bar for each spike plotted against the time it was recorded, and Part C shows the EEG. At the bottom (D) are the best-fit templates for each EEG cycle. A tick mark is plotted above the EEG and below the template to indicate the computed beginning of each cycle. In order to highlight the measured phase for each of the spikes, they are replotted in B as horizontal bars against the phase angle as the vertical axis.

The EEG phase of firing was determined relative to the location of the animal on the track and, separately, to the time from the beginning of the place field. The location on the maze was assessed by dividing the 1.5 m track into 256 bins of 0.58 cm each (the camera system pixel size). The time of each spike into the field was taken as the time after the animal crossed the point identified as the field onset (10% of maximum firing rate).

The correlation of the unit-EEG phase with each of the variables was determined by linear regression, or equivalently by finding the values of "m" and "b" that minimize

$$\Sigma_N(\phi - (mx + b))^2$$

for the N data pairs (x, ϕ). The standard approach cannot be used because the phase (ϕ) is periodic (360° = 0°), and large ϕ values would mistakenly be treated as far away from small ϕ values. Figure 3A contains an example data set, with the firing phase of each spike from a typical complex spike cell plotted against the position of the animal at the time of the spike. Since the phase is periodic, the data are actually distributed on the surface of the unit cylinder, which is constructed by joining the two dashed lines in the figure.

Conventional least-squares minimization with respect to m and b cannot be performed on these data, so the best-fit line was found using exhaustive search. The distance of the data from 72,000 different lines was tested, and the best-fit line was selected. Due to the rotational symmetry of the unit cylinder, the value for b must be between 0° and 360°, and in this analysis values for b were selected in steps of one degree. The slope of the line (m) took on values ranging from 10 rotations in the clockwise direction over the length of the cylinder to 10 rotations in the counterclockwise direction, in steps of ± 0.01 turns. The distance between the data and the model was computed for each of the lines, and the best-fit line was selected. The data were replotted (as in Fig. 3B) with 360° added or subtracted from data points to unwrap them from the unit cylinder. It was then possible to compute the Pearson correlation coefficient for each data set.

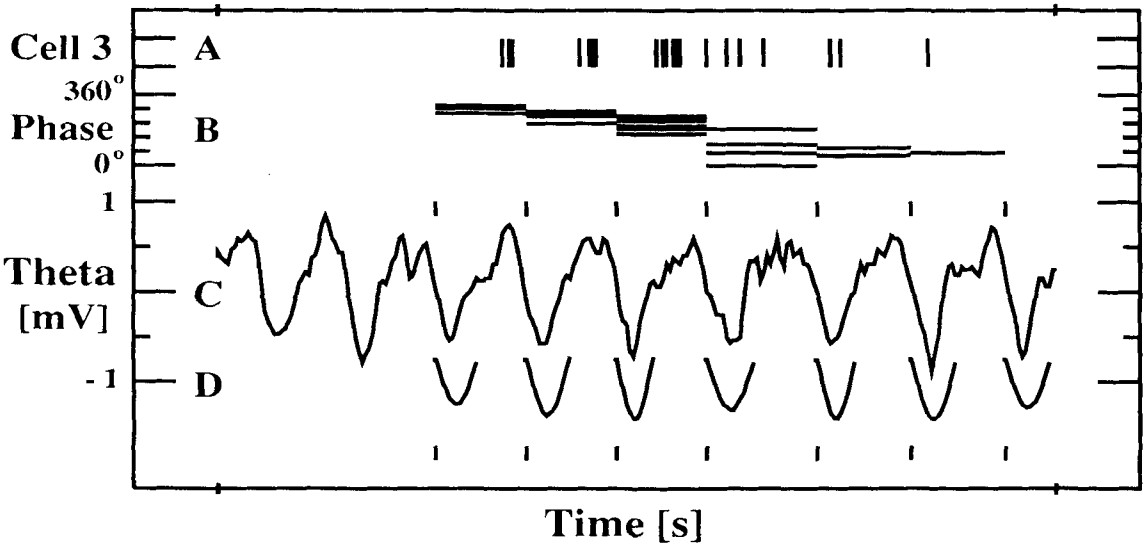

Fig. 2. Extraction of the firing phase shift for each spike during a single run through the field of a CA3 place cell on the linear track. (A) Each firing of cell 3 as a single vertical line during the 1 second of data. (B) Phase of each spike relative to the theta cycle within which it falls as a horizontal line. (C) Hippocampal theta activity recorded at the same time as the single unit. (D) Result of the theta template matching algorithm. Note that the amplitude and the time between onsets of each template match varies to fit the variations in the theta. The small vertical ticks above the electroencephalogram (EEG) and below the template fits mark the beginning of each theta cycle. The cell clearly fires six bursts of spikes during this run through the place field. Comparison of each burst with the concomitant theta wave shows that each successive burst fires on an earlier part of the theta. This is shown clearly by the descending staircase of the phase correlates in B. EEG voltage in C is +1 to −1 mV. Total time between marks on the x axis is 1 second.

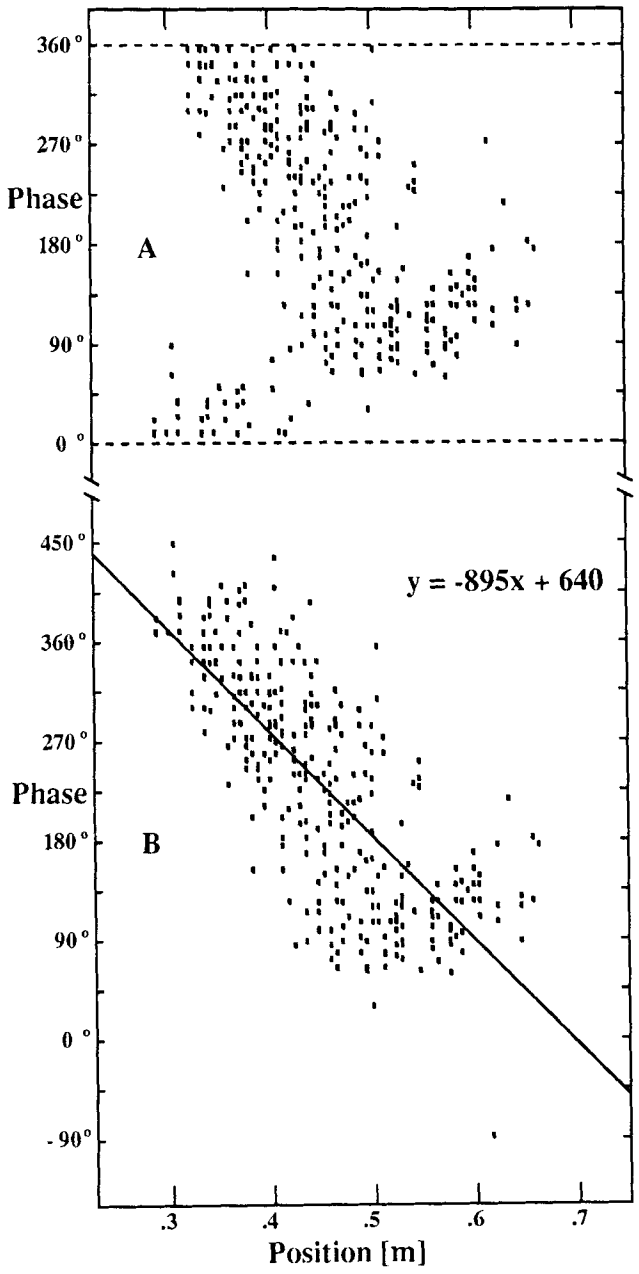

Fig. 3. Demonstration of the effect of the data mapping procedure to find the best-fit line to periodic phase data for cell 8. (A) Each spike location plotted against the phase of the theta wave. The spikes at the beginning of the field between 0.3 and 0.4 m on the track have clearly wrapped around the 0°/360° line and fall in the lower phase range. (B) Data pattern that results from the application of the unwrapping program. Imagine that the graph of A has been cut along the dotted line and rolled into a unit cylinder. The cylinder is rotated until a single straight line can be drawn through the data points. Many of the points in the left lower part of the graph have been wrapped to the left upper quadrant, and it is clear that a straight line provides a good fit to these data.

Electrode localization

After the final recording session, the electrodes were left in place for at least 1 day before the animal was sacrificed. Animals were deeply anesthetized with pentobarbital sodium (Lethobarb 0.7 mL/kg, Duphan) and perfused with saline followed by 10% formol saline. The brains were left in formol saline for several weeks and then sectioned every 50 μm in the sagittal plane and stained with cresyl violet. The location of unit clusters was reconstructed from the number of turns above the deepest penetration, from their relation to the major cell layers as determined by the amount of background multiple unit activity, and from the EEG sharp waves and the high-frequency ripple activity recorded at the same site (see O'Keefe and Nadel, 1978; Buzsaki et al., 1983).

RESULTS

Basic observations

Data were collected from three rats at eight electrode placements that were observed to have at least one cell firing on the maze during the recording session. From these 8 multiunit clusters, 19 cells were isolated in the analysis phase: 15 were classified as complex spike cells, 3 as theta cells, and 1 as unclassified, on the basis of wave shape and pattern of firing on the linear track. Here we report only the data from the 15 complex spike cells. The location of each of these units within the hippocampus is given in Table 1 together with other statistics. There were 11 CA1 and 4 CA3 complex spike cells. Of the 15 complex spike cells, 14 had a single localized region of firing on the track as the animal ran in one direction but failed to fire above the 10% threshold rate along the rest of the track or in the opposite direction. One complex spike cell fired in both directions on the track but in symmetrical locations rather than in the same place. There were therefore 16 sets of runs from 15 complex spike cells available for the phase analysis.

Place fields of the place cells

Figure 4 shows the 16 firing fields of the 15 place cells plotted as one-dimensional spatial histograms. Within each of the eight clusters there were one (three clusters), two (three clusters), or three (two clusters) cells with fields on the linear track. Our impression was that this was a small percentage of the complex spike cells under the electrode, several of which had fields on the holding box, but no attempt was made to quantify this. As can be seen in Figure 4, each field consisted of a single block of firing over a limited extent of the maze with virtually no firing outside this region. Some cells did show a small amount of firing during large irregular activity in the goal area, but this was eliminated by the run selection procedure as described in Materials and Methods. The length of the fields varied from 19 cm to 80 cm but did not appear to be normally distributed. Rather there appeared to be one group of fields of approximately 28 cm (12 bins) and another group of larger fields of approximately 61 cm (26 bins). Whether these represent single and double instances of a quantal field size cannot be concluded from the present small sample. The average firing rates in the fields varied from 3.3 spikes · s^{-1} to 28.5 spikes · s^{-1}, with a population mean

Table 1. Quantitative Summary of Phase Shift Results

Cell	Location	Firing Rate (spikes·s^{-1})	Field Size (bins)	Correlation (position)	Correlation (time in field)	Start Phase	End Phase	Phase Change	Slope (degrees/m)	Intercept (degrees)
1	1-CA1	10.4	11	.59	.21	390.3	102.7	287.6	−1116.0	1527.5
2	2-CA3	8.1	17	.68	.37	383.1	32.1	351.0	−880.8	888.8
3	2-CA3	24.1	10	.56	.40	344.8	157.8	187.0	−796.8	1158.8
4	3-CA1	14.8	13	.73	.50	437.4	82.8	354.6	−1164.0	887.0
5	4-CA1	21.0	23	.67	.52	193.5	−5.9	199.4	369.6	−99.0
6	4-CA1	17.5	21	.52	.11	250.5	101.2	149.3	−302.4	474.5
7	4-CA1	8.8	10	.65	.60	308.6	6.0	302.6	−1291.2	384.1
8	5-CA1	28.5	15	.76	.25	378.4	63.4	315.0	−895.2	640.8
9	6-CA1	11.8	26	.74	.67	442.5	120.0	322.5	528.0	−34.9
10	6-CA1	8.3	10	.80	.35	381.6	95.1	286.5	1221.6	−1266.1
11	6-CA1	7.0	14	.46	.54	405.3	305.8	99.5	−302.4	735.8
12	7-CA3	15.4	8	.57	.22	266.3	71.8	194.5	1036.8	−986.0
13	7-CA3	6.0	12	.78	.61	334.2	6.2	328.0	1166.4	−717.8
14	8-CA1	3.3	16	.76	.55	205.9	−64.0	269.9	720.0	−814.7
15	8-CA1	11.2	34	.70	.54	224.5	−24.1	248.6	312.0	−49.7
15b	8-CA1	4.7	29	.54	.37	215.0	−9.5	224.5	−328.8	450.7

The location column contains the cluster number and hippocampal region. The firing rate is averaged over the place field. 1 bin = 2.34 cm. The correlation (position) is the Pearson correlation coefficient of the phase vs. the location on the track, while the correlation (time) is the phase vs. the time after the start of the field. The start phase and end phase are taken from the best-fit line at the two ends of the place field. The phase change is the difference between the start and end phases, and the slope and intercept are the parameters of the best-fit line to the data.

of 12.6 ± 3.7. The field locations covered the entire maze, but there appeared to be a concentration of field centers around 0.5 m and around 1.2 m.

Phase correlate of the place cells

Figures 2, 5, and 6 show examples of the phase shift phenomenon. Figure 2 shows that the CA3 cell 3 fired a series of six bursts through the field, with the midpoint of each burst falling at a successively earlier stage of the concomitant theta cycle. On average, the number of spikes within each burst increased toward the middle of the field and then decreased as the animal exited from the field, but this was not invariable from trial to trial. In some cells the phase shift was reduced towards the exit of the field. Further examples of the phenomenon are shown in Figures 5 and 6, where the recordings from place cells 2 and 3 are depicted during four individual runs from the left to the right. In Figure 5 the runs are plotted against a time axis and in Figure 6 the same data are plotted against a position axis. Cell 2 fired in the center of the track, and cell 3 fired towards the right end of the track just at the edge of the goal area (see Fig. 4 for the fields). Neither fired above the threshold when the rat ran in the opposite direction. Also shown is the EEG taken from the dentate region just below the hippocampal fissure and the speed of the rat during the run. For this set of recordings, the location of the food in the righthand goal area was moved from run to run in order to prevent the animal from using its location as a cue to place field firing. This had the effect of causing the rat to slow down and search in the righthand goal area on some runs, causing large variations in the total run times. Two recordings (A and D) shown in Figure 5 were taken during uninterrupted runs from left to right, and two (B and C) portray runs during which the rat slowed or stopped at some point in the run. In C the rat stopped just at the edge of the cell 3 field, and in B it paused for a few seconds just inside the edge of the field.

Inspection of the relationship of each firing burst to the ongoing EEG theta activity shows the phase-shift phenomenon. In each cell the first spike burst occurred just after the positive peak of the theta as the rat entered the field, and moved forward in time (precessed) with each successive burst. The temporal length of the burst train and the temporal relationship between the burst trains in the two cells varied from run to run, depending on the speed at which the rat ran down the track. Furthermore, the theta phase of the spike bursts bore no apparent relation to the time at which they occurred.

In contrasting Figure 5 with the plot of the same data against position along the track in Figure 6, it is clear that the firing for each cell shows a systematic relationship to position across runs, as do the relationships between the cells, despite the large differences in lapsed time between them from one run to the next. Note also that the phase-shift phenomenon appears to show a relationship to the position on the track. For example, in run B the animal stopped just inside the field of cell 3 and searched at this point for almost 2 seconds (16 θ cycles, see Fig. 5), yet when forward movement resumed, the phase was appropriate for that position on the maze and shifted appropriately for the rest of the run.

In order to quantify the phase-shift phenomenon, the theta waves were modeled with sinusoids and each spike in the field firing burst was assigned a phase correlate relative to the modeled wave. In order to assess the relationship of this phase to spatial aspects of behavior, the phase of each spike was correlated with the animal's location on the maze. Figure 7A shows this correlation for place cell number 10 (see Fig. 4 for field), which was recorded from the CA1 region (EEG from 300 μm deeper in the CA1 field). It is clear

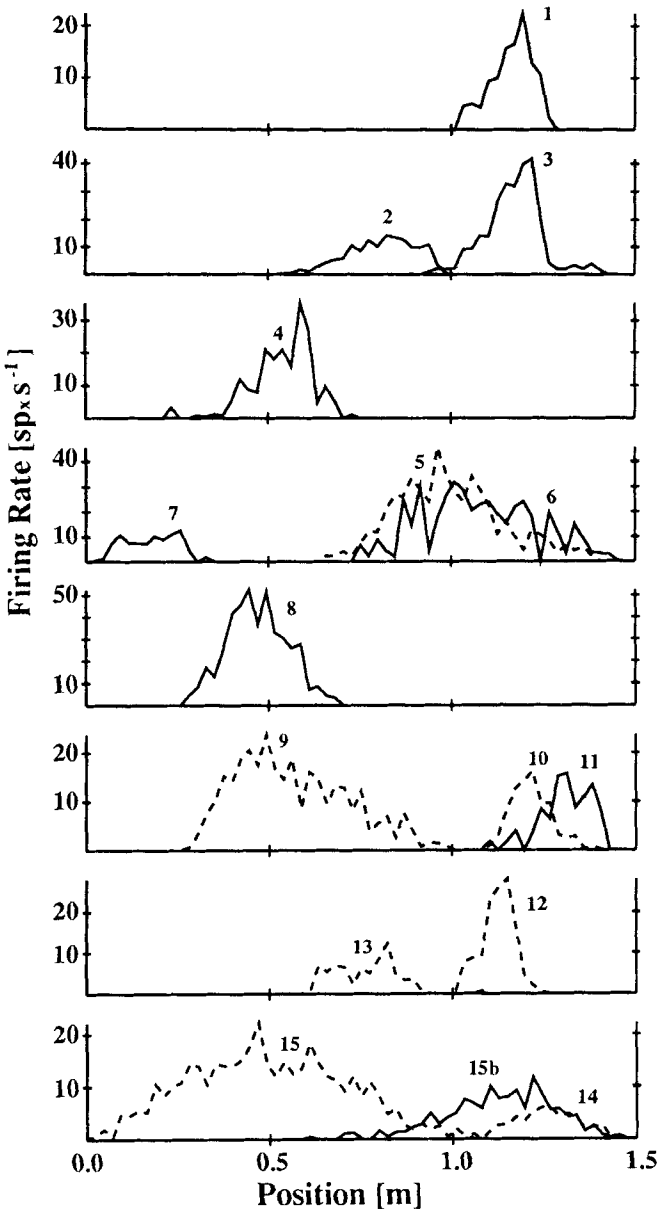

Fig. 4. Place field location for each of the complex spike cells. The data are organized in eight clusters, one for each of the recording sessions. Each field is labeled as in Table 1. The solid lines are rate maps from cells that fire on runs from left to right, and the dashed lines are rate maps from cells that fire on runs from right to left.

that there is a good correlation with the location of the animal.

One simple explanation of the phase-shift phenomenon is that the positional correlate is secondary to a temporal correlate, that is, that each cell burst shifts by a fixed part of a theta cycle once the place field is entered, irrespective of the animal's speed (see Discussion). In order to test this possibility, we looked at the correlation of the phase with time after entry into the field and compared it with the phase versus position correction. Figure 7C shows the result of this analysis for cell 10. It is clear that the scatter of the spike phase versus time is greater than for phase versus position.

The application of these analyses to the set of 16 direction/runs substantiated the above findings. Table 1, column 5 shows the correlations of all the cells to location on the track and column 6 to the time into the place field. In 15 of 16 cases the temporal correlation is lower than the corresponding spatial correlation, and this is reflected in the large difference between the averages (0.66 ± 0.026 SEM vs. 0.42 ± 0.041 SEM).

All place cells had phase shifts (range, 100°–355°) that were related to the animal's location on the maze. Figure 8 gives a graphic illustration of all of the fits and Table 1, column 5 gives the numerical details. For a given cell, the phase shift began at approximately the same point of the theta cycle on each run, but this point varied from cell to cell. For all the data sets, the phase shift was in the same direction. The best-fit lines in Figure 8 that have a negative slope correspond to cells that fire when the rat runs from left to right, while the lines with a positive slope are from cells that fire during movement in the other direction. As noted above, the relative phase among the EEG recording electrodes was not systematically recorded, so no significance should be attributed to the absolute phase measures. There did not appear to be a relationship between the field sizes or the firing rate and the slope of the phase shift.

DISCUSSION

Our results show that hippocampal place cells often fire with a series of bursts as the animal runs through the place field and that the phase relationship between the spike bursts and the EEG theta activity changes systematically within the field. In this section we discuss how this finding relates to previous results, the possible mechanisms responsible for producing the phase-shift effect, and the role that this phase shift might play in synaptic modification within the hippocampus.

Our results suggest a different picture from those reported previously (Buzsaki et al., 1983; Fox et al., 1986; Otto et al., 1991), where data were averaged and which reported only the overall preferred phase that the complex cells have to the theta activity. Fox et al. (1986) studied the firing correlates of hippocampal cells while the rat was running on a treadmill, and hence was unlikely to be in the place field. They found that the main correlate of the CA3/4 complex spike cells on the treadmill was after the peak of the dentate theta positivity (at 19°), while the CA1 complex spike cell phase correlate was before the theta positivity (at 325°). In contrast, Buzsaki et al. (1983) found peaks at an earlier phase (270°) for CA3/4 and a later phase (0°) for CA1. Otto et al. (1991) found that the phase correlate of the first spike in each burst varied from 275° to 312° depending on the task. Our results cannot be compared directly to these previous findings, since we did not refer each unit to the same theta. It is clear from our results, however, that at least in the place field, the identification of a single phase correlate does not adequately describe the firing pattern of the cells. Instead, one must establish the phase as it changes across the field. We prefer to characterize the phenomenon in terms of starting phase and total phase shift. Our data suggest that within any one cluster the phase

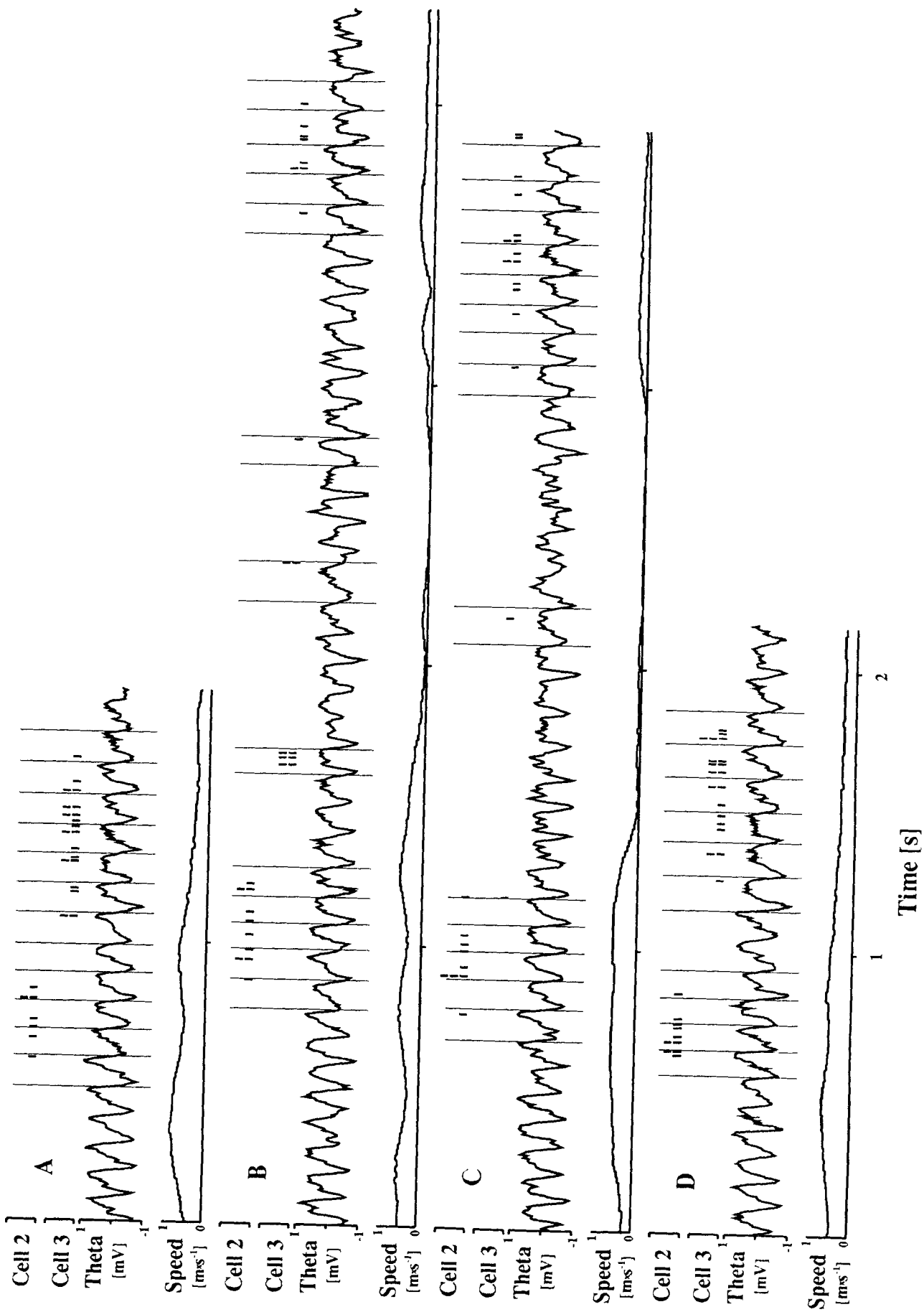

onsets appear to be roughly the same, but we cannot say anything about the phase relations between different parts of the hippocampus. The results have important implications for understanding the way in which place is represented by the complex spike firing.

Representation of spatial location

The results suggest that the place cells have a much higher spatial resolution on narrow-armed mazes than had previously been thought (on the basis of experiments using firing rate as the sole measure of spatial information). Not only does the phase information provide a second measure of location that may be independent of firing rate, but in one sense it is superior. If we assume that most place fields are symmetrical and approximately Gaussian, then there is an ambiguity for any given level of firing rate as to whether the animal is on one side of the center of the field or the other. No such ambiguity exists with the phase correlate, since it is a monotonic function of location, each phase identifying a unique location. Whether this also applies to open-field situations in which the place cell firing is nondirectional must remain moot at this point (see Muller et al., 1987). It is possible that the phase angle is the primary index of location and that the firing rate is secondary, or even carrying additional information. Since the background firing tends to occur at a constant phase, the start and end of the place field could be defined using the phase of the spikes. Furthermore, the readout of hippocampal activity could be performed by phase-sensitive detectors. These downstream cells would be able to distinguish between activity in the field and either spontaneous out-of-field activity or spikes that occur during large irregular activity.

Mechanism underlying the phase shift

The main features of the phenomenon that need to be accounted for are: (1) the bursting pattern of the place cell firing through the field; (2) the precession of this bursting pattern relative to the EEG theta waves; (3) the onset of the bursting at a constant point of the theta waves as the animal enters the field; (4) the bell shape of the firing field and the tendency for the peak firing to occur in the middle of the phase shift; and (5) the confinement of the phase shift to 360° or less.

The phase shift for each of the 15 cells fits well to a straight line, which can be explained only if the bursting rate of each cell has a higher frequency than the corresponding EEG theta rhythm. Figure 9 shows this effect for cell 3 where the autocorrelation of the cell is compared with the theta period taken from the EEG recorded as the animal ran through the field (i.e., excluding the data recorded outside the field). It is clear that the peak value of the theta period is slightly shifted to the right of the cell autocorrelation function, suggesting that the latter has a higher frequency than the former.

In our discussion of mechanisms, we begin with the simplest models in which the effects are due to simple oscillations within a single cell and then proceed to more complex mechanisms. The most obvious possibility is that the cell acts as a simple oscillator. The oscillator could be turned on for as long as the inputs exceed the firing threshold (a voltage-controlled oscillator, see Hoppensteadt, 1986), or it might be initiated by a single driving impulse and decay independently. If the frequency of the oscillator were slightly higher than the theta frequency, then there would be a progressive shift forward of the firing relative to the theta as the animal moved through the field. While this mechanism accounts for the phase precession, it fails to account for two facts: (1) the field firing always begins at a particular phase of the theta cycle, and (2) the phase shift is restricted to 360° or less. The first constraint would require that the afferent inputs be timed to begin consistently at a fixed theta phase, while the second constraint would require that they be restricted to a limited duration.

With either simple oscillator, dynamical properties would be the major determinant of the temporal sequence of spikes, and these would occur relatively independently of the animal's subsequent location or speed. It follows that the time after the beginning of the oscillation (or what is equivalent, the first burst in the field) should be a better predictor of the cell behavior than the rat's location within the field. Since we have shown that, in general, the correlation between phase and time after field entry is considerably worse than the correlation between phase and position (Table 1), we believe these simple models are unlikely to be adequate.

The deficiencies of the single oscillator model can be overcome if there are at least two different rhythmic generators operating within the system and they are oscillating *at slightly different frequencies*. If we make the further assumption that both of these oscillations are impinging on each cell, the generation of the firing pattern within the place field might be due to the interference patterns set up by the two oscillations (see O'Keefe, 1985). There are several ways this could happen. First, let us consider the possibility that both oscillations are continuously impinging on the cell but that throughout most of an environment they are roughly of equal amplitude and of opposite phase, canceling each other out or at best resulting in the occasional spike at the peak of one of the phases. Within the field, however, the frequency of one of the oscillators increases slightly relative to the other. Under

Fig. 5. Four runs (A–D) during the recording of cells 2 and 3 from cluster 2 (CA3). The top two rows in each graph show the firing of each cell as a single vertical line. Aligned multiple vertical lines for the same cell indicate instances where the cell fired too rapidly for the individual spikes to be shown on this slow time base. The third row in each graph shows the concurrent EEG taken from an electrode at the level of the hippocampal fissure. Positive voltage is up. Calibrations are ± 1 mV. The fourth row shows the speed of movement of the rat on the track. The x axis for all graphs is time in seconds. Each run begins after the animal leaves the left goal and ends before it enters the right one. Runs A and D show fast uninterrupted runs, while B and C show runs where the rat slowed and paused at some point in the run. Note that the firing pattern of each cell shows the phase shift on each run, beginning near the positive peak of the theta and moving to progressively earlier phases with each cycle. Note also that the temporal relations between the firing of the two cells can vary markedly, depending on the animal's behavior.

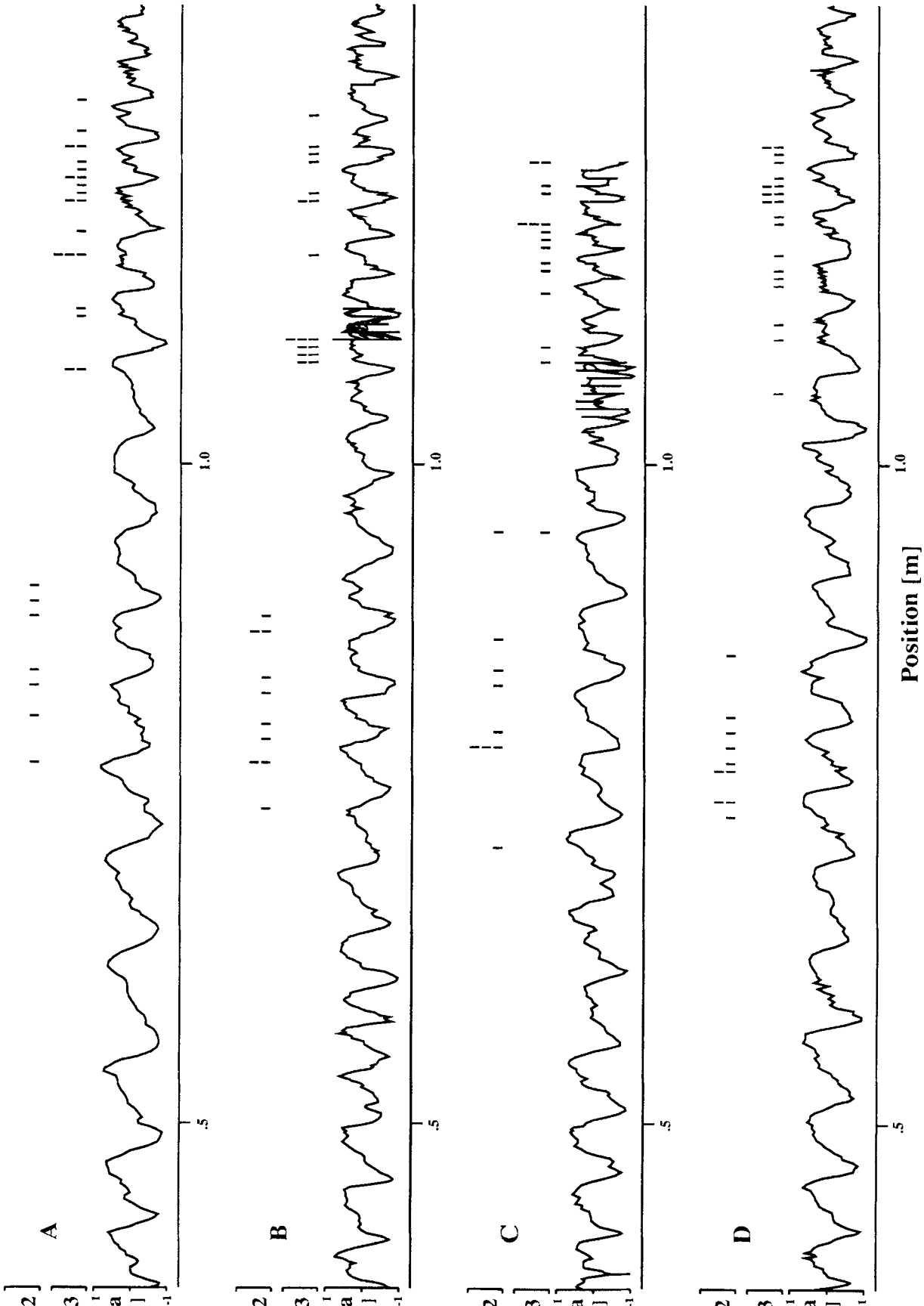
A
B
C
D
Cell 2
Cell 3
Theta [mV]
1
-1
.5
1.0
Position [m]

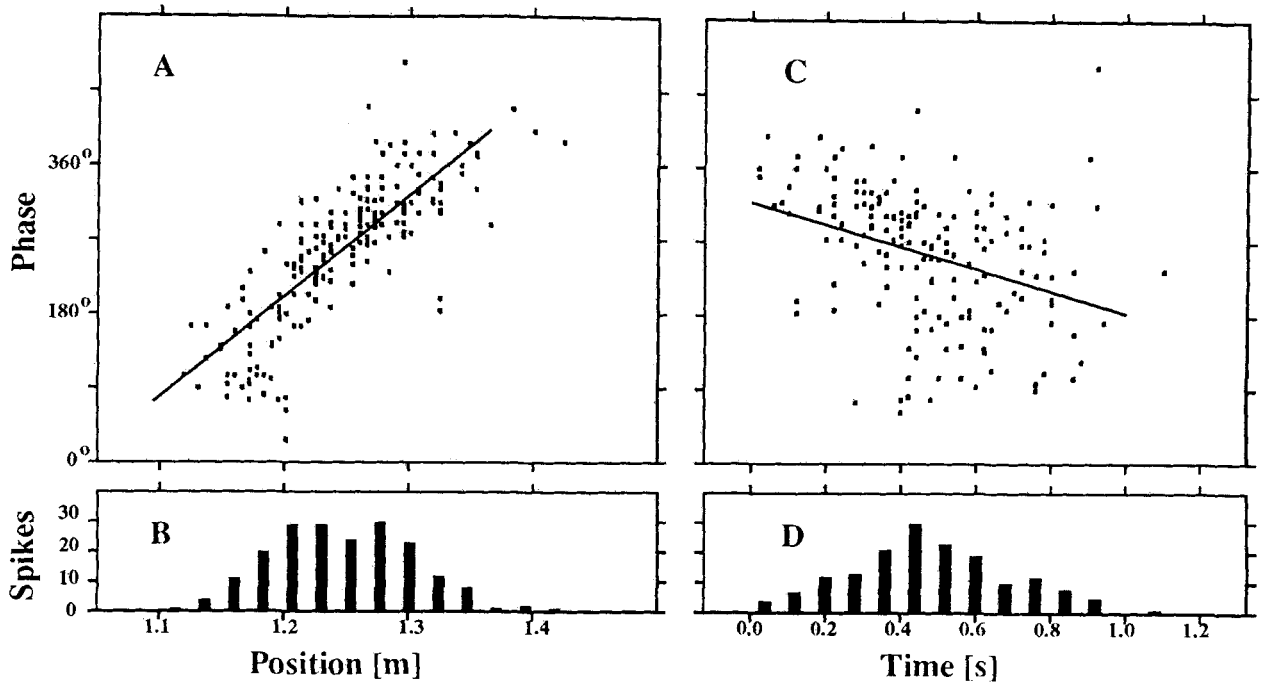

Fig. 7. (A) Plot of theta phase of cell 10 (CA1) (y axis) against position on the linear track (x axis). Hippocampal EEG was recorded from an electrode 300 μm deeper in the CA1 field than the unit recording electrode. Positive voltage up. 0°/360° phase was selected as described in the text. (B) Number of spikes at each location on the track during the 41 runs used to construct the plot in A. (C) Phase data from the same runs plotted against time after field entry. (D) Number of spikes at each time after entry into field. Note that the correlation of phase with position ($r = 0.80$) is much better than the correlation with time into field ($r = 0.35$). Position calibration in B is for A and B, time calibration in D is for C and D.

these conditions, the output of the cell, evinced in its firing pattern, will be represented by the interference pattern resulting from the summation of the two waves. Figure 10 illustrates this effect for waves of frequencies 9 and 11 Hz. The wave packet produced is governed by the general wave equation for the summation of two spatiotemporal sinusoids of differing frequencies:

$$y = 2a \cos[0.5(k_1 + k_2)x - 0.5(\omega_1 + \omega_2)t] \cdot \sin[0.5(k_1 - k_2)x - 0.5(\omega_1 - \omega_2)t]$$

where k is the spatial propagation number of each wave and ω is the angular frequency of the temporal component.

As can be seen, there are four components to this equation, two spatial and two temporal. The average difference of the two frequencies (e.g., the $0.5(\omega_1 - \omega_2)$ term) determines the period of the wave packet envelope (in the example, 1 Hz), while the average of the two frequencies (e.g., the $0.5(\omega_1 + \omega_2)$ term) gives rise to the oscillations within the wave packet (in the example, 10 Hz). The present suggestion is that the envelope of the wave packet determines the place field, while the amplitude of the beat oscillations determines the firing rate within the wave packet. Note, for example, that the amplitude of the oscillations within the wave packet rises and falls, giving rise to the bell-shaped profile of the place field. Furthermore, if one assumes that one of the input waves is reflected in the frequency of the gross EEG theta, the model also predicts the precession of the phase shift. Note how the peak of the wave packet progressively moves to earlier phases of the B wave.

In this model, the temporal components relate to the frequencies of the two waves in time, but the spatial components relate to the tracing of the waves across an environment as the animal moves through the environment. This opens up the interesting possibility that the field size, which is given by the difference term, can be maintained constant despite changes in the speed of movement of an animal through the environment (the k component) by compensating changes in the frequency of the waves (the ω component). A brief correlation between the rat running speed and the theta frequency at the onset of a movement has been reported (Whishaw and Vanderwolf, 1973), but no long-lasting correlation during con-

Fig. 6. The same data shown in Figure 5, but with the spikes and EEG voltages plotted against the rat's position on the maze as the x axis. The phase shift is still apparent, but now in addition the firing fields of the cells are in greater alignment. The distortion of the EEG record towards the end of runs B and C is due to the superposition of many theta cycles in the same location as the rat's speed falls to zero. The record in C is truncated because the rat turned at this point and ran in the opposite direction. Note the overlap of the spikes in the two cells in C at approximately 0.9 m, where the end of the cell 2 field overlaps the beginning of the cell 3 field. Calibration ± 1 mV for the EEG. The x axis scale is in meters.

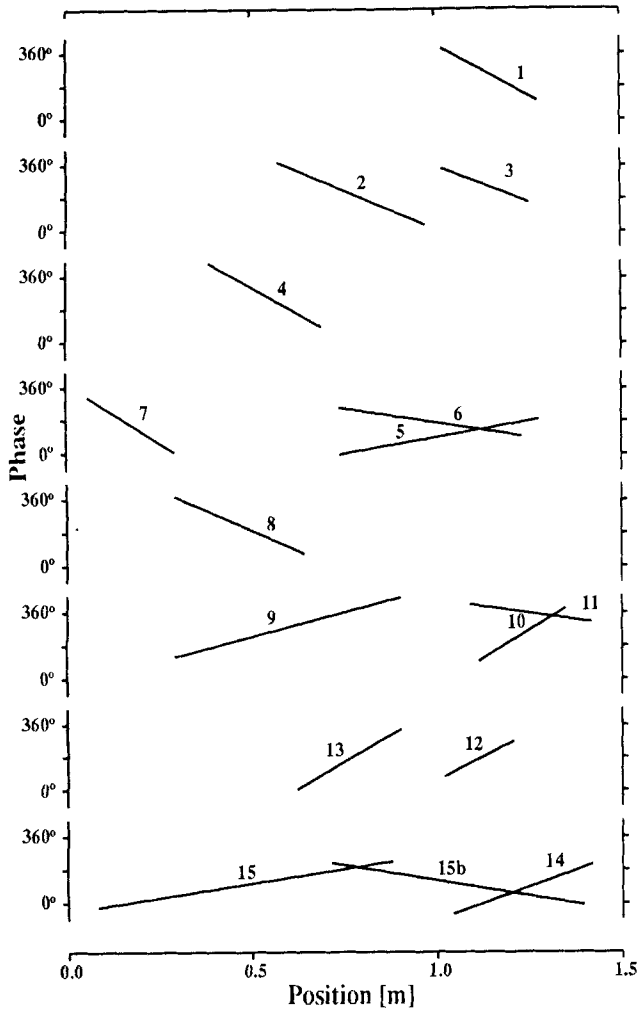

Fig. 8. Phase profiles for the 15 place cells. Each of the eight sections represents one cluster. Phase shift is always in the descending direction, so that shifts that ascend from left to right are from cells that fired as the rat ran from right to left. See Figure 4 for the corresponding fields.

tinuous running on a treadmill was found. The prediction remains to be tested during normal movements through an environment.

The notion that each pyramidal cell acts as an oscillator, or as the summator of input oscillations, raises many questions for future consideration. The first concerns the origin of the two frequencies. One possibility is that they are both external to the hippocampus and that the hippocampal cells are essentially passive devices whose sole function is to sum their inputs. The alternative view is that the hippocampal cells act as oscillators, perhaps as voltage-controlled oscillators (Hoppensteadt, 1986), whose dynamics translate input voltages to output frequencies. This leads to questions such as whether each cell has a fixed natural frequency, or alternatively whether the frequency varies with the environment. The phase-shift versus position curves for some cells are best approximated by straight lines, suggesting that the second input frequency in the field has a fixed difference from the EEG theta. In others (e.g., Fig. 2) the curves may have a more sigmoidal shape, which would be more in keeping with a second frequency that rises, peaks, and then falls. In some curves there is evidence of a lessening of the phase precession as the animal exits the field, clear evidence of a frequency reduction. There are several suggestions as to how the membrane and channel properties of single cells might enable them to oscillate either as individuals (Llinas, 1988) or when embedded in networks (Traub et al., 1989).

Alternative simple explanations of the phase shift are difficult to identify. For example, it might be thought that the depolarization of the cell increased as the animal approached the center of the field and then decreased as it moved out again, and that this interacted with a depolarizing phase of the theta rhythm. This would explain the increased firing rate into the field and to some extent the precession forward, since the cell might tend to fire at an earlier point in time when it was more depolarized. It fails, however, to account for the continued precession as the animal runs out of the field coupled with a decrease in firing rate unless an additional mechanism is invoked. But this additional mechanism must be one that allows for an increased excitation to account for the con-

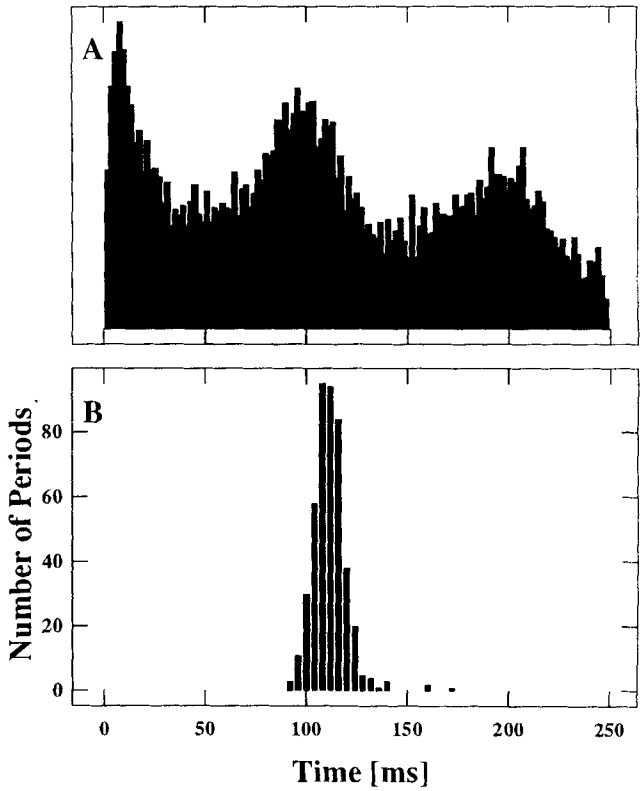

Fig. 9. Comparison of the spike period and the EEG wave period. (A) Autocorrelation of the spike data from cell 3. The y axis scale is in arbitrary units. Bin width is 2 ms. (B) Interval histogram of the EEG periods derived from the sine wave fit program. Only theta waves during unit firing were used. Bin width is 4 ms. The y axis shows the number of instances of each theta period within the place field. Note that the peak of the theta period in B is shifted to the right of the autocorrelation peak in A.

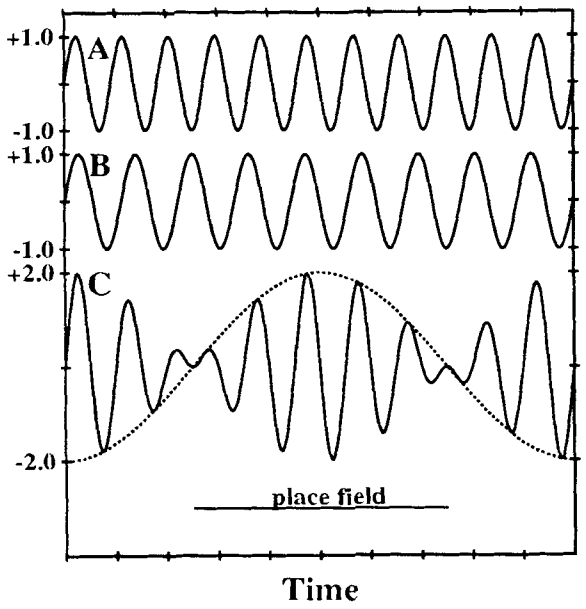

Fig. 10. Interference pattern model of place field formation. Two sinusoids of the same amplitude but different frequencies (A, B) will sum to produce the pattern shown in (C). The top (A) has a frequency of 11 Hz, the assumed rate at which the data are projected to the cell. The middle (B) has a frequency of 9 Hz, read from the EEG interval data. The bottom wave (C) oscillates with an average frequency of 10 Hz and a beat frequency of 1 Hz. The firing in the place field is determined by the compound wave, with the amplitude of the positive peaks determining the average phase relative to the EEG wave. The positive phase of the slow beat wave (dotted line) determines the temporal extent of the field.

tinued precession and a decreased excitation to account for the decreased number of spikes per cycle.

Synaptic changes

It is widely believed that learning involves synaptic modifications and that one important variable for this is the temporal relationship between different afferents onto a postsynaptic cell and between the pre- and postsynaptic activations (Collingridge and Bliss, 1987). Recently, interest has developed in the relationship between the optimal parameters for synaptic enhancement and the firing patterns observed in freely moving animals (Larson and Lynch, 1989; Otto et al., 1991). In this section, we explore the ways in which the pattern of firing associated with the phase shift places interesting conditions on the temporal relations between synaptically coupled cells and thus on the possibility that synaptic connection between place cells will be strengthened (or reduced) in a given environment. The first possibility is that the timing of the presynaptic input relative to the theta cycle is important. Pavlides et al. (1988) reported good long-term potentiation if the electrically induced afferent barrages impinged on the cells during the positive phase of the dentate EEG and no change or a decrease in synaptic efficacy if the inputs occurred at the negative phase. It is possible that afferent inputs to the cell at some phases in the theta cycle could be most effective in producing synaptic enhancement. This might mean that only spikes occurring at one part of the place field (e.g., at the trailing edge of the field) would be effective in strengthening the synapses onto the downstream cells.

The second possibility is that the absolute phase of theta at which the burst occurs is less relevant than the relative timing of the spikes in the two cells. Here we examine that temporal relationship and ask whether the spatial relationship between their place fields influences their synaptic coupling. Muller et al. (1991) have assumed that the synaptic coupling strength falls off as a monotonic function of the time between place cell activations, and therefore that cells with neighboring fields will be more strongly coupled than those with distant ones. In contrast, the phase-shift phenomenon suggests that the relationship between synaptic coupling and place field location is more complex.

Let us assume for the sake of illustration that the effective time window for synaptic modification is less than one theta cycle and further that all of the cells in a region of the hippocampus (e.g., the CA3 field) have phase shifts that begin at the same phase of theta. It follows that the synaptic coupling function between connected cells of similar field sizes will not be a monotonic function of distance. Cells with completely overlapping fields will experience the strongest coupling, since the spike trains will coincide throughout each run through the fields (ignoring the delays introduced by the conduction and excitatory postsynaptic potential rise times). As the place field centers are shifted relative to each other, the time separating the bursts in one train will shift relative to those in the second spike train. At the point where one field center becomes shifted to lie on the periphery of the second field (50% overlap of the fields), the temporal spike patterns will occur 180° out of phase with each other, and a maximum temporal disparity will be reached. As the fields separate even further, however, the spike bursts in one train will approach the bursts of the next theta cycle in the second train, and the temporal disparity will begin to decrease. The next maximum would occur at the point at which the fields were completely separated and abutting, but this maximum would not reach the same strength as the complete overlap condition, since only the spike bursts at the beginning and end of the trains would occur contemporaneously. The synaptic strengthening function on this model would have two peaks: a large one when complete overlap occurs, and a smaller one when fields are edge-abutting. If long-term depression exists, and can be shown to occur when two spike trains have a 180° phase relation, it would enhance the above effect.

In summary, the temporal firing properties of the hippocampal complex spike of the cells appear to contribute importantly to the way that these cells represent the animal's location. Furthermore, the phase shift may provide one of the basic mechanisms by which information is processed and stored within the hippocampus.

ACKNOWLEDGMENTS

The authors thank Drs. Andrew Speakman and Natalya Shvyrkova for scientific advice and technical assistance, Clive Parker for technical help, and Maureen Cartwright for editorial advice. The work was supported by the Medical Research Council (U.K.). Preliminary reports have been published in *Society of Neuroscience Abstracts* 18:707 and in the

Abstracts of the 9th National Meeting of the Brain Research Association at Nottingham, April 1992, in *Neuroscience Letters Supplement* 42:S45.

References

Berger TW, Rinadli PC, Weisz DJ, Thompson RF (1983) Single-unit analysis of different hippocampal cell types during classical conditioning of rabbit nictitating membrane response. J Neurophysiol 50:1197–1219.

Bland BH (1986) The physiology and pharmacology of hippocampal formation theta rhythms. Prog Neurobiol 26:1–54.

Buzsaki G, Leung LWS, Vanderwolf CH (1983) Cellular bases of hippocampal EEG in the behaving rat. Brain Res Rev 6:139–171.

Collingridge GL, Bliss TVP (1987) NMDA receptors: their role in long-term potentiation. Trends Neurosci 10:288–293.

Eichenbaum H, Kuperstein M, Fagan A, Nagode J (1986) Cue-sampling and goal-approach correlates of hippocampal unit activity in rats performing an odor discrimination task. J Neurosci 7:716–732.

Fox SE, Ranck JB (1975) Localization and anatomical identification of theta and complex spike cells in dorsal hippocampal formation of rats. Exp Neurol 49:299–313.

Fox SE, Wolfson S, Ranck JB (1986) Hippocampal theta rhythm and the firing of neurons in walking and urethane anesthetized rats. Exp Brain Res 62:495–508.

Hoppensteadt FC (1986) An introduction to the mathematics of neurons. Cambridge: Cambridge University Press.

Larson J, Lynch G (1989) Theta pattern stimulation and the induction of LTP: the sequence in which synapses are stimulated determines the degree to which they potentiate. Brain Res 489:49–58.

Llinas RR (1988) The intrinsic electrophysiological properties of mammalian neurons: insights into central nervous function. Science 242:1654–1664.

McNaughton BL, O'Keefe J, Barnes CA (1983a) The stereotrode, a new technique for simultaneous isolation of several single units in the central nervous system from multiple unit records. J Neurosci Meth 8:391–397.

McNaughton BL, Barnes CA, O'Keefe J (1983b) The contributions of position, direction and velocity to single unit activity in the hippocampus of freely-moving rats. Exp Brain Res 52:41–49.

Muller RU, Kubie JL, Ranck JB (1987) Spatial firing patterns of hippocampal complex-spike cells in a fixed environment. J Neurosci 7:1935–1950.

Muller RU, Kubie JL, Saypoff R (1991) The hippocampus as a cognitive graph (Abridged version). Hippocampus 1:243–246.

O'Keefe J (1976) Place units in the hippocampus of the freely moving rat. Exp Neurol 51:78–109.

O'Keefe J (1985) Is consciousness the gateway to the hippocampal cognitive map? A speculative essay on the neural basis of mind. In: Brain and mind (Oakley DA, ed), pp 59–98. London: Methuen.

O'Keefe J, Conway DH (1978) Hippocampal place units in the freely moving rat: why they fire where they fire. Exp Brain Res 31: 573–590.

O'Keefe J, Conway DH (1980) On the trail of the hippocampal engram. Physiol Psychol 8:229–238.

O'Keefe J, Dostrovsky J (1971) The hippocampus as a spatial map: preliminary evidence from unit activity in freely moving rats. Brain Res 34:171–175.

O'Keefe J, Nadel L (1978) The hippocampus as a cognitive map. Oxford: Clarendon Press.

O'Keefe J, Speakman A (1987) Single unit activity in the rat hippocampus during a spatial memory task. Exp Brain Res 68:1–27.

Olton DS, Branch M, Best PJ (1978) Spatial correlates of hippocampal unit activity. Exp Neurol 58:387–409.

Otto T, Eichenbaum H, Wiener SI, Wible CG (1991) Learning-related patterns of CA1 spike trains parallel stimulation parameters optimal for inducing hippocampal long-term potentiation. Hippocampus 1: 181–192.

Pavlides C, Greenstein YJ, Grudman M, Winson J (1988) Long-term potentiation in the dentate gyrus is induced preferentially on the positive phase of theta-rhythm. Brain Res 439:383–387.

Ranck JB (1973) Studies on single neurons in dorsal hippocampal formation and septum in unrestrained rats. Part 1. Behavioral correlates and firing repertoires. Exp Neurol 41:461–531.

Recce ML, O'Keefe J (1989) The tetrode: a new technique for multiunit extracellular recording. Soc Neurosci Abstr 15:1250.

Recce ML, Speakman A, O'Keefe J (1991) Place fields of single hippocampal cells are smaller and more spatially localised than you thought. Soc Neurosci Abstr 17:484.

Sinclair BR, Seto MG, Bland BH (1982) Theta-cells in CA1 and dentate layers of hippocampal formation: relations to slow-wave activity and motor behavior in the freely-moving rabbit. J Neurophysiol 48:1214–1225.

Stanton PK, Sejnowski TJ (1989) Associative long-term depression in the hippocampus induced by hebbian covariance. Nature 339: 215–218.

Traub RD, Miles R, Wong RKS (1989) Model of the origin of rhythmic population oscillations in the hippocampal slice. Science 243: 1319–1325.

Vanderwolf CH (1969) Hippocampal electrical activity and voluntary movement in the rat. Electroencephalogr Clin Neurophysiol 26: 407–418.

Whishaw IQ, Vanderwolf CH (1973) Hippocampal EEG and behaviour changes in amplitude and frequency of RSA (theta rhythm) associated with spontaneous and learned movement patterns in rats and cats. Behav Biol 8:461–484.